

## Syntheses, Structures, and Magnetic Properties of $\text{Np}_3\text{S}_5$ and $\text{Np}_3\text{Se}_5$

Geng Bang Jin,<sup>†,‡</sup> S. Skanthakumar,<sup>‡</sup> Richard G. Haire,<sup>§</sup> L. Soderholm,<sup>\*,‡</sup> and James A. Ibers<sup>\*,†</sup>

<sup>†</sup>*Department of Chemistry, Northwestern University, Evanston, Illinois, 60208-3113, United States,* <sup>‡</sup>*Chemical Science and Engineering Division, Argonne National Laboratory, Argonne, Illinois 60439, United States, and*

<sup>§</sup>*Chemical Sciences Division, Oak Ridge National Laboratory, Oak Ridge, Tennessee 37831, United States*

Received September 18, 2010

Black prisms of  $\text{Np}_3\text{Q}_5$  (Q = S, Se) have been synthesized by the stoichiometric reactions between Np and Q at 1173 K in a CsCl flux. The structures of these compounds were characterized by single-crystal X-ray diffraction methods. The  $\text{Np}_3\text{Q}_5$  compounds are isostructural with  $\text{U}_3\text{Q}_5$ . The structure of  $\text{Np}_3\text{Q}_5$  is constructed from layers of  $\text{Np}(1)\text{Q}_8$  distorted bicapped trigonal prisms that share faces with each other on *bc* planes. Each  $\text{Np}(1)\text{Q}_8$  layer further shares  $\text{Q}(2)$  edges with two adjacent identical neighbors to form a three-dimensional framework. The space inside each channel within this framework is filled by one single edge-sharing  $\text{Np}(2)\text{Q}_7$  distorted 7-octahedron chain running along the *b* axis. Magnetic susceptibility measurements show that  $\text{Np}_3\text{S}_5$  and  $\text{Np}_3\text{Se}_5$  have antiferromagnetic orderings at 35(1) and 36(1) K, respectively. Above the magnetic ordering temperatures, both  $\text{Np}_3\text{S}_5$  and  $\text{Np}_3\text{Se}_5$  behave as typical Curie–Weiss paramagnets. The effective moments obtained from the fit of the magnetic data to a modified Curie–Weiss law over the temperature range 70 to 300 K are 2.7(2)  $\mu_B$  ( $\text{Np}_3\text{S}_5$ ) and 2.9(2)  $\mu_B$  ( $\text{Np}_3\text{Se}_5$ ).

### Introduction

Binary actinide chalcogenides  $\text{An}_x\text{Q}_y$  (An = actinide; Q = S, Se, Te) exist in a variety of crystal structures and chemical compositions with An/Q ratios between 1:1 and 1:5.<sup>1–3</sup> As a result, they exhibit a wide range of electronic and magnetic properties. Among these, 20  $\text{Np}_x\text{Q}_y$  compounds with formulas of  $\text{NpQ}$  (Q = S, Se, Te),  $\text{Np}_3\text{Q}_4$  (Q = S, Se, Te),  $\text{Np}_2\text{Q}_3$  (Q = S, Se, Te),  $\text{Np}_3\text{Q}_5$  (Q = S, Se),  $\text{NpQ}_2$  (Q = S, Te),  $\text{Np}_2\text{Q}_5$  (Q = S, Se), and  $\text{NpQ}_3$  (Q = S, Se, Te) have been identified.<sup>2,4</sup> Most of these compounds have been characterized only by powder X-ray diffraction analyses, and their physical properties have not been fully studied. It is interesting that binary neptunium chalcogenides exhibit a very rich structural chemistry compared to binary neptunium oxides, which comprise only two stable phases,  $\text{NpO}_2$  and  $\text{Np}_2\text{O}_5$ .<sup>2</sup> This difference arises in part because of the propensity of

chalcogens to form Q–Q bonds. In these  $\text{Np}_x\text{Q}_y$  compounds formal oxidation states of +3 and +4 are found for Np; in contrast aqueous species exhibit stable oxidation states for Np of +4, +5, +6, and, under very alkaline conditions, +7.<sup>5</sup>

The  $\text{An}_3\text{Q}_5$  (An = U, Np; Q = S, Se) compounds are of particular interest because they are borderline between the metal-like actinide-rich compounds and the semiconducting chalcogen-rich phases. Both charge balance and crystal structures suggest that these compounds contain  $\text{An}^{3+}$  and  $\text{An}^{4+}$  in a ratio of 2:1, consistent with the interpretation of X-ray photoelectron spectroscopic measurements on comparable U compounds and with <sup>237</sup>Np Mössbauer spectroscopic measurements.<sup>4,6–12</sup> The chemical formula can thus be written as  $(\text{An}^{3+})_2(\text{An}^{4+})(\text{Q}^{2-})_5$ .  $\text{U}_3\text{S}_5$  and  $\text{U}_3\text{Se}_5$  have been extensively studied.<sup>6,7,11,13–16</sup> They crystallize in the space group *Pnma* with  $\text{U}^{3+}$  and  $\text{U}^{4+}$  cations occupying the

\*To whom correspondence should be addressed. E-mail: LS@anl.gov (L.S.), ibers@chem.northwestern.edu (J.A.I.). Phone +1 630 252 4364 (L.S.), +1 847 491 5449 (J.A.I.). Fax: +1 847 491 2976 (J.A.I.).

(1) Grenthe, I.; Drozdowski, J.; Fujino, T.; Buck, E. C.; Albrecht-Schmitt, T. E.; Wolf, S. F. In *The Chemistry of the Actinide and Transactinide Elements*, 3rd ed.; Morss, L. R., Edelstein, N. M., Fuger, J., Eds.; Springer: Dordrecht, The Netherlands, 2006; Vol. 1, pp 253–698.

(2) Yoshida, Z.; Johnson, S. G.; Kimura, T.; Krsul, J. R. In *The Chemistry of the Actinide and Transactinide Elements*, 3rd ed.; Morss, L. R., Edelstein, N. M., Fuger, J., Eds.; Springer: Dordrecht, The Netherlands, 2006; Vol. 2, pp 699–812.

(3) Manos, E.; Kanatzidis, M. G.; Ibers, J. A. In *The Chemistry of the Actinide and Transactinide Elements*, 4th ed.; Morss, L. R., Edelstein, N. M., Fuger, J., Eds.; Springer: Dordrecht, The Netherlands, 2010; Vol. 6, pp 4005–4078.

(4) Thévenin, T.; Jové, J.; Pagès, M. *Hyperfine Interact.* **1984**, 20, 173–186.

(5) Williams, C. W.; Blaudeau, J. P.; Sullivan, J. C.; Antonio, M. R.; Bursten, B.; Soderholm, L. *J. Am. Chem. Soc.* **2001**, 123, 4346–4347.

(6) Potel, M.; Brochu, R.; Padiou, J.; Grandjean, D. *C. R. Seances Acad. Sci., Ser. C* **1972**, 275, 1419–1421.

(7) Moseley, P. T.; Brown, D.; Whittaker, B. *Acta Crystallogr.* **1972**, B28, 1816–1821.

(8) Marcon, J.-P. *C. R. Seances Acad. Sci., Ser. C* **1967**, 265, 235–237.

(9) Marcon, J.-P. *Commis. Energ. At. [Fr]*, *Rapp.* **1969**, CEA-R-3919, 1–99.

(10) Damien, D.; Damien, N.; Jové, J.; Charvillat, J. P. *Inorg. Nucl. Chem. Lett.* **1973**, 9, 649–655.

(11) Kohlmann, H.; Beck, H. P. *J. Solid State Chem.* **2000**, 150, 336–341.

(12) Thévenin, T.; Jové, J.; Pagès, M.; Damien, D. *Solid State Commun.* **1981**, 40, 1065–1066.

(13) Suski, W.; Reizer-Netter, H. *Bull. Acad. Pol. Sci., Ser. Sci. Chim.* **1974**, 22, 701–707.

(14) Noël, H.; Prigent, J. *Phys. B+C* **1980**, 102, 372–379.

Wyckoff positions 8d (site symmetry 1) and 4c (site symmetry  $m$ ), respectively.<sup>6,7</sup>  $U_3S_5$  is a semiconductor and ferromagnet ( $T_c = 29$  K) that displays a large negative magnetoresistance effect.<sup>11,14,16</sup>  $U_3Se_5$  is also a semiconductor; it orders ferromagnetically below 24 K.<sup>13,15</sup>  $U_3Te_5$  adopts a different structure type.<sup>17</sup> In contrast,  $Np_3Q_5$  (Q = S, Se) have been identified only from powder X-ray diffraction data from which it was deduced that they are isostructural with  $U_3S_5$ .<sup>4,8–10,12</sup> Electrical resistivity measurements on a cold-pressed powder pellet have shown that  $Np_3S_5$  is a semiconductor, whereas  $Np_3Se_5$  exhibits semimetallic behavior.<sup>18</sup> There are no reliable magnetic data for  $Np_3Q_5$ , although <sup>237</sup>Np Mössbauer measurements at 4.2 K have suggested that the magnetic moment of Np should order at low temperatures.<sup>4,12</sup>

The syntheses of powder samples of  $Np_3Q_5$  have included direct reactions between Np or  $NpH_x$  and Q, or thermal decomposition of  $NpQ_3$ .<sup>4,8,10,12</sup> Here we report the syntheses of large single crystals of  $Np_3S_5$  and  $Np_3Se_5$  by a different route. These crystals have enabled us to examine more thoroughly their structures and magnetic properties.

## Experimental Section

**Syntheses.** S (Alfa-Aesar, 99.99%), Se (Cerac 99.999%), and CsCl (Strem Chemicals, 99.999%) were used as received. Brittle pieces of high-purity arc-melted <sup>237</sup>Np metal (ORNL) were crushed and used in these syntheses.

**Caution!**<sup>237</sup>Np and any ingrown daughter products are  $\alpha$ - and  $\beta$ -emitting radioisotopes and as such are considered a health risk. Its use requires appropriate infrastructure and personnel trained in the handling of radioactive materials. The procedures we use for the syntheses of Np compounds have been described.<sup>19</sup>  $Np_3S_5$  and  $Np_3Se_5$  were prepared through the reactions of 0.086 mmol (0.020 g) of Np, 0.15 mmol (S: 0.005 g, Se: 0.012 g) of Q, and 0.090 g of CsCl flux. The reactants were loaded into fused-silica ampules in an Ar-filled glovebox and then flame-sealed under vacuum. The reaction mixtures were heated in a furnace to 1173 K in 32 h, held at 1173 for 4 days, cooled to 773 K in 5.5 days, held at 773 K for 2 days, and then cooled further to 298 K over 6 h. The reaction products were washed with water and dried with acetone. Large black prisms of  $Np_3Q_5$  up to 0.8 mm in length were the major product. The yields of  $Np_3Q_5$  were about 90 wt %. A few small black plates of  $NpOQ$  were also found.<sup>20</sup> Single crystals of  $Np_3Q_5$  obtained in these reactions were used in the determination of their crystal structures. Magnetic measurements were performed on ground single crystals.

**Structure Determinations.** Single-crystal X-ray diffraction data for  $Np_3S_5$  and  $Np_3Se_5$  were collected with the use of graphite-monochromatized Mo K $\alpha$  radiation ( $\lambda = 0.71073$  Å) at 100 K on a Bruker APEX2 diffractometer.<sup>21</sup> The crystal-to-detector distance was 5.106 cm. Data were collected by a scan of  $0.3^\circ$  in  $\omega$  in groups of 600 frames at  $\varphi$  settings of  $0^\circ$ ,  $90^\circ$ ,  $180^\circ$ , and  $270^\circ$ . The exposure time was 20 s/frame. The collection of

**Table 1.** Crystal Data and Structure Refinements for  $Np_3S_5$  and  $Np_3Se_5$ <sup>a,b</sup>

	$Np_3S_5$	$Np_3Se_5$
Fw	871.30	1105.80
<i>a</i> (Å)	11.7435(6)	12.2863(5)
<i>b</i> (Å)	8.0479(4)	8.3499(4)
<i>c</i> (Å)	7.4108(4)	7.7583(3)
<i>V</i> (Å <sup>3</sup> )	700.40(6)	795.92(6)
$\rho_c$ (g/cm <sup>3</sup> )	8.263	9.228
$\mu$ (cm <sup>-1</sup> )	455.51	616.39
<i>R</i> ( <i>F</i> ) <sup>c</sup>	0.0183	0.0222
<i>R</i> <sub>w</sub> ( <i>F</i> <sub>o</sub> <sup>2</sup> ) <sup>d</sup>	0.0405	0.0474

<sup>a</sup> For both structures, orthorhombic system, space group = *Pnma*, *Z* = 4,  $\lambda = 0.71073$  Å, and  $T = 100(2)$  K. <sup>b</sup> From room-temperature X-ray diffraction powder data in refs 9 and 10: *a* = 11.71(2) Å, *b* = 8.07(1) Å, *c* = 7.42(1) Å for  $Np_3S_5$ ; *a* = 12.24(2) Å, *b* = 8.43(1) Å, *c* = 7.75(1) Å for  $Np_3Se_5$ . No structural parameters were presented; it was deduced that these compounds were isostructural with  $U_3S_5$ . <sup>c</sup>  $R(F) = \sum ||F_o| - |F_c|| / \sum |F_o|$  for  $F_o^2 > 2\sigma(F_o^2)$ . <sup>d</sup>  $R_w(F_o^2) = \{ \sum w(F_o^2 - F_c^2)^2 / \sum wF_o^4 \}^{1/2}$  for all data.  $w^{-1} = \sigma^2(F_o^2) + (qF_o^2)^2$  for  $F_o^2 \geq 0$ ;  $w^{-1} = \sigma^2(F_o^2)$  for  $F_o^2 < 0$ .  $q = 0.0152$  for  $Np_3S_5$ , 0.0101 for  $Np_3Se_5$ .

intensity data as well as cell refinement and data reduction were carried out with the use of the program APEX2.<sup>21</sup> Absorption corrections for  $Np_3Se_5$  (face indexed) and  $Np_3S_5$ , as well as incident beam and decay corrections were performed with the use of the program SADABS.<sup>22</sup> The structures were solved with the direct-methods program SHELXS and refined with the least-squares program SHELXL.<sup>23</sup> The program STRUCTURE TIDY<sup>24</sup> was used to standardize the positional parameters. Additional experimental details are given in Table 1 and in the Supporting Material.

**Powder X-ray Diffraction Measurements.** Powder X-ray diffraction patterns were collected with a Scintag XGEN-4000 diffractometer with the use of Cu K $\alpha$  radiation ( $\lambda = 1.5418$  Å).

**Magnetic Susceptibility Measurements.** The magnetic susceptibility data were collected with the use of a Quantum Design MPMS 7 SQUID magnetometer on 2.3 mg of  $Np_3S_5$  and 3.4 mg of  $Np_3Se_5$ , encapsulated to comply with safety regulations. To optimize purity, the samples used for susceptibility measurements were obtained by grinding enough small ( $\sim 5$   $\mu$ g) single crystals to provide adequate signal statistics. The signal from the empty sample-holder, which accounted for as much as 90% of the signal at room temperature, was measured separately and subtracted directly from the total magnetic response. Susceptibility data were subsequently corrected for Langevin diamagnetism.<sup>25,26</sup> Variable field measurements, performed at 5 and 300 K to a maximum of 2 and 5 T, respectively, appeared linear over the entire field range thus enabling data acquisition at higher fields. Field-cooled and zero-field-cooled data showed no significant evidence for simple ferromagnetic ordering down to 5 K. Variable temperature experiments were carried out between 5 and 320 K, under applied fields of 0.0025, 0.01, 0.05, 0.2, 0.5, and 1 T. These data provided the same results within experimental error, notably after field cycling, thus confirming the sample stability to orientation effects that can possibly arise with powdered samples.

## Results and Discussion

**Syntheses.** Stoichiometric reactions of Np and Q resulted in 90% yields of  $Np_3Q_5$  (Q = S, Se) and several  $NpOQ$

(15) Shlyk, L.; Troc, R.; Kaczorowski, D. *J. Magn. Magn. Mater.* **1995**, *140–144*, 1435–1436.

(16) Shlyk, L.; Troc, R. *Phys. B* **1999**, *262*, 90–97.

(17) Tougait, O.; Potel, M.; Noël, H. *J. Solid State Chem.* **1998**, *139*, 356–361.

(18) Blaise, A.; Damien, D.; Mulak, J. *Phys. Status Solidi A* **1982**, *72*, k145–k148.

(19) Wells, D. M.; Jin, G. B.; Skanthakumar, S.; Haire, R. G.; Soderholm, L.; Ibers, J. A. *Inorg. Chem.* **2009**, *48*, 11513–11517.

(20) Jin, G. B.; Raw, A. D.; Skanthakumar, S.; Haire, R. G.; Soderholm, L.; Ibers, J. A. *J. Solid State Chem.* **2010**, *183*, 547–550.

(21) APEX2 Version 2009.5–1 and SAINT Version 7.34a Data Collection and Processing Software; Bruker Analytical X-Ray Instruments, Inc.: Madison, WI, 2009.

(22) SMART Version 5.054 Data Collection and SAINT-Plus Version 6.45a Data Processing Software for the SMART System; Bruker Analytical X-Ray Instruments, Inc.: Madison, WI, 2003.

(23) Sheldrick, G. M. *Acta Crystallogr., Sect. A: Found. Crystallogr.* **2008**, *64*, 112–122.

(24) Gelato, L. M.; Parthé, E. *J. Appl. Crystallogr.* **1987**, *20*, 139–143.

(25) Boudreaux, E. A.; Mulay, L. N. *Theory and Applications of Molecular Paramagnetism*; Wiley International: New York, 1976.

(26) Fournier, J. M. *Struct. Bonding (Berlin)* **1985**, *59–60*, 127–196.

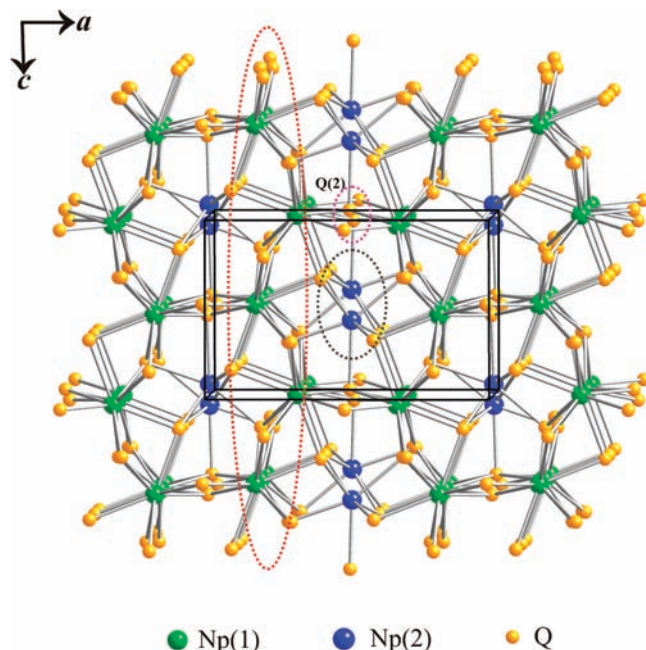
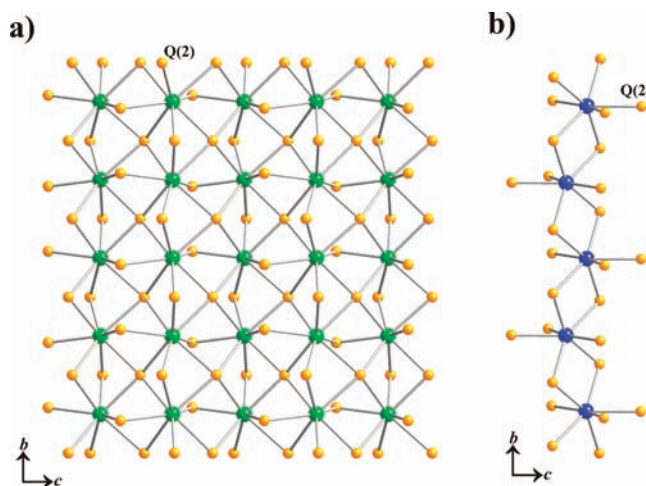
**Table 2.** Selected Interatomic Distances (Å) for  $\text{Np}_3\text{S}_5$  and  $\text{Np}_3\text{Se}_5$ 

distance	$\text{Np}_3\text{S}_5$	$\text{Np}_3\text{Se}_5$
Np(1)–Q(1)	2.8652(9)	2.9922(5)
Np(1)–Q(1)	2.9000(9)	3.0214(5)
Np(1)–Q(2)	2.9049(8)	3.0295(5)
Np(1)–Q(2)	2.9230(9)	3.0617(5)
Np(1)–Q(3)	2.9489(9)	3.0761(5)
Np(1)–Q(3)	3.024(1)	3.1522(5)
Np(1)–Q(4)	2.8826(9)	3.0062(5)
Np(1)–Q(4)	2.926(1)	3.0395(5)
Np(2)–Q(1) × 2	2.6527(9)	2.7738(5)
Np(2)–Q(1) × 2	2.7213(9)	2.8415(5)
Np(2)–Q(2)	2.852(1)	2.9770(7)
Np(2)–Q(3)	2.756(1)	2.8895(7)
Np(2)–Q(4)	2.777(1)	2.8964(7)
Np(1)···Np(1)	4.0103(3)	4.1660(4)
Np(1)···Np(2)	4.1892(3)	4.3674(3)
Np(2)···Np(2)	4.1681(2)	4.3331(2)

crystals.<sup>20</sup> The oxide layer on the surface of the Np metal and etching of the silica ampoules were possible oxygen sources.

$\text{Np}_3\text{S}_5$  crystals were first obtained from the reaction of Np, Fe, and S with a CsCl flux at 1173 K. They were also found as significant byproducts in other neptunium sulfide reactions, for example, the reactions of Np with  $\text{P}_2\text{S}_5$  and S at 973, 1173, and 1248 K, respectively.<sup>27</sup> This indicates that  $\text{Np}_3\text{S}_5$  has a high stability. In contrast, similar reactions of U, Fe, S, and CsCl at 1173 K<sup>28</sup> resulted in  $\beta\text{-US}_2$ <sup>29</sup> and  $\text{US}_3$ <sup>30</sup> as byproducts, both of which contain  $\text{U}^{4+}$ . In fact, they are the most common binary  $\text{U}_x\text{S}_y$  compounds found in solid-state reactions that involve uranium and sulfur. Clearly, the sulfide chemistries of Np and U differ significantly.

**Structures.** Our single-crystal structures for  $\text{Np}_3\text{S}_5$  and  $\text{Np}_3\text{Se}_5$  agree with those deduced from powder studies but are much more precise (Tables 1 and 2). These compounds are isostructural with  $\text{U}_3\text{Q}_5$ , crystallizing in the space group  $Pnma$  (Figure 1). The structure includes two crystallographic unique metal positions, Np(1) at the Wyckoff position 8d (site symmetry 1) and Np(2) at the Wyckoff position 4c (site symmetry  $.m.$ ). Each Np(1) cation is connected to eight Q anions in a distorted bicapped trigonal prism whereas the Np(2) cation is surrounded by seven Q anions in a highly distorted 7-octahedron (Figure 2). Np(1)Q<sub>8</sub> polyhedra share faces with each other along the  $b$  and  $c$  axes to form two-dimensional layers (circled in red in Figure 1) and further share Q(2) edges (circled in purple in Figure 1) to form a three-dimensional channel structure. The space inside each channel is filled by one single edge-sharing Np(2)Q<sub>7</sub> chain running down the  $b$  axis (circled in black in Figure 1). The connectivities within each layer of Np(1)Q<sub>8</sub> and single chain of Np(2)Q<sub>7</sub> are shown in Figure 2a and Figure 2b, respectively. The condensed packing pattern of these Np(1)Q<sub>8</sub> bicapped trigonal prisms is not common. Similar layers of Gd(1)S<sub>8</sub> bicapped trigonal prisms occur in the structure of  $\text{Gd}_2\text{S}_3$ ; however, there are no further con-

**Figure 1.** Structure of  $\text{Np}_3\text{S}_5$  and  $\text{Np}_3\text{Se}_5$ .**Figure 2.** Depictions of an individual Np(1)Q<sub>8</sub> layer (a) and Np(2)Q<sub>7</sub> chain (b) viewed down the  $b$  axis.

tions between these Gd(1)S<sub>8</sub> layers.<sup>31</sup> Generally, bicapped trigonal prisms share trigonal faces to form chains and then only share edges between them, such as the  $\text{NpS}_8$  polyhedra in  $\text{Np}_2\text{S}_3$ <sup>32</sup> and the  $\text{AnQ}_8$  polyhedra in  $\text{AnMQ}_3$  ( $\text{An} = \text{U}, \text{Th}; \text{M} = \text{Sc}, \text{Fe}, \text{Mn}; \text{Q} = \text{S}, \text{Se}, \text{Te}$ ).<sup>33</sup>

Selected interatomic distances for  $\text{Np}_3\text{S}_5$  and  $\text{Np}_3\text{Se}_5$  are listed in Table 2. That the Np(1)–Q distances are generally longer than the Np(2)–Q distances is consistent with Np(1) having a formal oxidation state of +3 and Np(2) being +4. The Np–Q distances are about 0.01–0.02 Å shorter than those in the corresponding U compounds,<sup>6,7</sup> owing to the actinide contraction. For example, Np(1)–S distances, which range from 2.8652(9) to 3.024(1) Å, may be compared to those of 2.872(3) to 3.033(3) Å for the U(1)–S distances in  $\text{U}_3\text{S}_5$ .<sup>6</sup>

(27) Jin, G. B.; Skanthakumar, S.; Haire, R. G.; Soderholm, L.; Ibers, J. A., unpublished results.

(28) Jin, G. B.; Ringe, E.; Long, G. J.; Grandjean, F.; Sougrati, M. T.; Choi, E. S.; Wells, D. M.; Balasubramanian, M.; Ibers, J. A. *Inorg. Chem.* **2010**, *49*, 10455–10467.

(29) Suski, W.; Gibinski, T.; Wojakowski, A.; Czopnik, A. *Phys. Status Solidi A* **1972**, *9*, 653–658.

(30) Noël, H. *J. Less-Common Met.* **1986**, *121*, 265–270.

(31) Prewitt, C. T.; Sleight, A. W. *Inorg. Chem.* **1968**, *7*, 1090–1093.

(32) Zachariasen, W. H. *Acta Crystallogr.* **1949**, *2*, 291–296.

(33) Narducci, A. A.; Ibers, J. A. *Chem. Mater.* **1998**, *10*, 2811–2823.

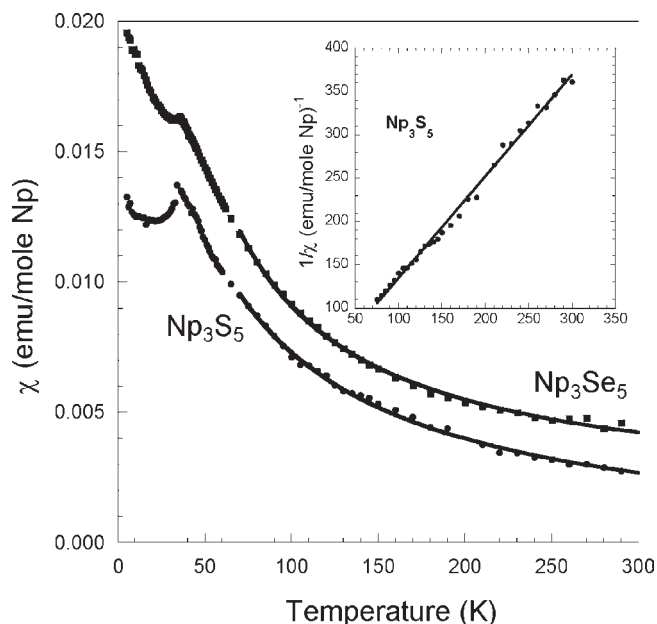


**Figure 3.**  $\chi$  versus  $T$  for  $\text{Np}_3\text{S}_5$  and  $\text{Np}_3\text{Se}_5$  under an applied field of 0.2 T. The solid line through the data above 70 K represents the best fit to the modified Curie–Weiss law. The inset shows  $1/\chi$  versus  $T$  for  $\text{Np}_3\text{S}_5$ .

The seven-coordinate  $\text{Np}^{4+}$  cations have  $\text{Np}(2)\text{--S}$  distances that range from 2.6527(9) to 2.852(1) Å; these are generally longer than those of 2.681(2) to 2.754(1) Å for the six-coordinate  $\text{Np}^{4+}$  cations in  $\text{AMNpS}_3$  ( $A = \text{K}, \text{Rb}, \text{Cs}; M = \text{Cu}, \text{Ag}$ )<sup>19</sup> and shorter than those of 2.889(2) and 2.9067(8) Å in the nine-coordinate  $\text{Np}^{4+}$  cations in  $\text{NpOS}$ .<sup>20</sup> Similarly the  $\text{Np}(2)\text{--Se}$  distances range from 2.7738(5) to 2.9770(7) Å; these are shorter than those of 3.0055(5) and 3.077(1) Å found for the nine-coordinate  $\text{Np}^{4+}$  cations in  $\text{NpOSe}$ .<sup>20</sup> The eight-coordinate  $\text{Np}^{3+}$  cations have  $\text{Np}(1)\text{--Se}$  distances that range from 2.9922(5) to 3.1522(5) Å; these are longer than those of 2.9330(6) to 3.1419(6) Å for the seven-coordinate  $\text{Np}^{3+}$  cations in  $\text{NpCuSe}_2$ .<sup>34</sup>

The empirical bond-valence analysis has been widely employed to estimate the formal oxidation states of metal atoms in a given compound. Such analyses depend on the availability of a large number of results for a given bond type. However, there are only a few  $\text{Np}\text{--S}$  and even fewer  $\text{Np}\text{--Se}$  distances available from single-crystal studies. A value of the necessary bond-valence parameter  $R_0$  of 2.57 was obtained from the  $\text{Np}\text{--S}$  distances in  $\text{KCuNpS}_3$ ,  $\text{RbCuNpS}_3$ ,  $\text{CsCuNpS}_3$ ,  $\text{KAgNpS}_3$ , and  $\text{CsAgNpS}_3$ ; these compounds contain  $\text{Np}^{4+}$ .<sup>19</sup> If we take into consideration the present  $\text{Np}(1)^{3+}\text{--S}$  and  $\text{Np}(2)^{4+}\text{--S}$  distances, the new average value of  $R_0$  is 2.56 for the six compounds  $\text{KCuNpS}_3$ ,  $\text{RbCuNpS}_3$ ,  $\text{CsCuNpS}_3$ ,  $\text{KAgNpS}_3$ ,  $\text{CsAgNpS}_3$ , and  $\text{Np}_3\text{S}_5$ . With this value of  $R_0$  the bond valences of  $\text{Np}(1)$  and  $\text{Np}(2)$  are calculated to be 3.03 and 4.45, respectively, in  $\text{Np}_3\text{S}_5$ . Because there are only three  $\text{Np}\text{--Se}$  distances known from single-crystal studies ( $\text{NpCuSe}_2$ <sup>34</sup> and the present  $\text{Np}_3\text{Se}_5$ ) it is not possible to perform similar calculations for  $\text{Np}\text{--Se}$  distances.  $\text{Np}\text{--Q}$  distances from  $\text{NpOQ}$ <sup>20</sup> compounds are not included in the current discussion, as they are affected

by the  $\text{Np}\text{--O}$  interactions. Obviously, more  $\text{Np}\text{--Q}$  distances would be needed to optimize the bond-valence parameters for  $\text{Np}\text{--Q}$  compounds.

**Magnetism.** As noted above, the structure of the  $\text{Np}_3\text{Q}_5$  compounds contains a  $\text{Np}^{3+}$  cation at Wyckoff position 8d (site symmetry 1) and a  $\text{Np}^{4+}$  cation at Wyckoff position 4c (site symmetry  $m$ ). If we assume Russell–Saunders coupling, then  $\text{Np}^{3+}$ , with a  $5f^4$  configuration, is a non-Kramers ion that, under the reduced site symmetry, may have a singlet ground state. In contrast,  $\text{Np}^{4+}$ , with a  $5f^3$  configuration, is a Kramers ion and as such will have a magnetic ground state irrespective of site symmetry.

Representative susceptibilities of  $\text{Np}_3\text{S}_5$  and  $\text{Np}_3\text{Se}_5$ , compared as  $\chi$  versus  $T$  in Figure 3, exhibit cusps in their susceptibilities at 35(1) and 36(1) K, respectively, evidence suggesting long-range magnetic ordering below those temperatures. With  $\text{Np}\cdots\text{Np}$  distances in both structures longer than 4.0 Å, well in excess of the Hill limit,<sup>35</sup> the observed ordering temperatures are consistent with the presence of localized moments. Previous studies on the magnetic susceptibility of  $\text{Np}_3\text{Se}_5$  found no evidence for magnetic ordering down to temperatures as low as 4.2 K,<sup>18,36</sup> however, note that the published figure in the previous study<sup>18</sup> does not include data for the temperature range 5 to 30 K, the range over which the cusp is observed in our data. In addition, a previous <sup>237</sup>Np Mössbauer study of  $\text{Np}_3\text{S}_5$  included spectra obtained at 77 and 4.2 K.<sup>12</sup> Both spectra indicated the presence of two distinct Np sites, with the isomer shifts identifying one as  $\text{Np}^{3+}$  and the other as  $\text{Np}^{4+}$ . The low-temperature spectrum is more complex, showing contributions from both internal electric and magnetic fields, a result consistent with but not proof of long-range magnetic order. Similar magnetic hyperfine fields were found at the two Np sites, indicating that both  $\text{Np}^{3+}$  and  $\text{Np}^{4+}$  may be participating in the magnetic ordering in  $\text{Np}_3\text{S}_5$ . In our magnetic susceptibility data the cusp for  $\text{Np}_3\text{S}_5$  is much more pronounced than that for  $\text{Np}_3\text{Se}_5$ , which may indicate only one sublattice is ordering in the latter material. For comparative interest,  $\text{NpSe}_3$ , which contains only  $\text{Np}^{4+}$ , orders ferromagnetically at 51 K with a second ordering at 18 K.<sup>18</sup> In contrast,  $\text{Np}_2\text{Se}_3$ , which contains exclusively  $\text{Np}^{3+}$ , shows no evidence of magnetic splitting in the Mössbauer data obtained at 4.2 K.<sup>4</sup> We assume the  $\text{Np}\cdots\text{Np}$  distances in these compounds are comparable to those in their isostructural uranium analogues.<sup>7,37,38</sup> The results from the Np compounds are expected because the low symmetries of the Np sites should yield singlet ground states for the  $\text{Np}^{3+}$  ions and magnetic doublets for the  $\text{Np}^{4+}$  Kramers ions. On the basis of these expectations, ordering in the  $\text{Np}_3\text{Q}_5$  compounds should be largely driven by the  $\text{Np}^{4+}$  sublattices.

(35) Hill, H. H. In *Plutonium 1970 and Other Actinides*; Miner, W. N., Ed.; The Metallurgical Society of the American Institute of Mining, Metallurgical, and Petroleum Engineers, Inc.: New York, 1970; Vol. 17, pp 2–19.

(36) Blaise, A.; Fournier, J. M.; Salmon, P.; Wojakowski, A. *Plutonium 1975 Other Actinides. Proceedings of the 5th International Conference on Plutonium and Other Actinides*, Baden Baden, Sept 10–13, 1975; Blank, H., Lindner, R., Eds.; North-Holland: Amsterdam, 1976; pp 635–640.

(37) Ben Salem, A.; Meerschaut, A.; Rouxel, J. C. *R. Acad. Sci., Sér. 2* **1984**, 299, 617–619.

(38) Samokhvalova, E. P.; Molchanov, V. N.; Tat'yanina, I. V.; Torchenkova, E. A. *Sov. J. Coord. Chem. (Engl. Transl.)* **1990**, 16, 683–687.

(34) Wells, D. M.; Skanthakumar, S.; Soderholm, L.; Ibers, J. A. *Acta Crystallogr., Sect. E: Struct. Rep. Online* **2009**, 65, i14.

**Table 3.** Magnetic Behaviors of  $\text{Np}_3\text{S}_5$  and  $\text{Np}_3\text{Se}_5$ <sup>a</sup>

	$\text{Np}_3\text{S}_5$	$\text{Np}_3\text{Se}_5$
$T_N$ (K)	35(1)	36(1)
$\mu_{\text{eff}}$ ( $\mu_B$ )	2.7(2)	2.9(2)
free ion (calc.) $\mu_{\text{eff}}$ ( $\mu_B$ )	3.03	3.03
$\theta$ (K)	-30(5)	-15(5)
$\chi_0$ ( $10^{-4}$ emu/mol)	3(3)	10(2)

<sup>a</sup>The data presented in Figure 3 were fit to a modified Curie–Weiss law over the temperature range 70 to 300 K.

Above the magnetic ordering at about 35 K, both  $\text{Np}_3\text{S}_5$  and  $\text{Np}_3\text{Se}_5$  behave as classic paramagnets. With the assumption of non-interacting spins, the data may be fit to a modified Curie–Weiss law:

$$\chi = C/(T - \theta) + \chi_0 \quad (1)$$

over the temperature range 70 to 300 K, where  $C$  is the Curie constant from which the effective moment is related by  $\mu_{\text{eff}} = (8C)^{1/2}$ ,  $\theta$  is the Weiss constant, representing either magnetic correlations or low-lying crystal-field states, and  $\chi_0$  is the temperature-independent paramagnetism (TIP), a term meant to account for itineracy (Pauli paramagnetism) or the influence of low-lying crystal-field states (van Vleck paramagnetism). The best fits yield the results shown in Table 3.

The effective moment is defined as  $\mu_{\text{eff}} = g(J(J+1))^{1/2}$ , where  $J$  is the Russell–Saunders full angular momentum.  $\text{Np}^{3+}$ , with  $J = 4$  ground level, has a free-ion moment of  $2.68 \mu_B$ , whereas  $\text{Np}^{4+}$ , with  $J = 9/2$  ground level, has a free-ion moment of  $3.62 \mu_B$ . The effective moments measured experimentally are slightly smaller than, or of the same magnitude as the full free-ion moment predicted from Hund's rules for a 2:1 ratio of  $\text{Np}^{3+}/\text{Np}^{4+}$ . This result confirms the presence of at least some  $\text{Np}^{4+}$ , because the free-ion moment from  $\text{Np}^{3+}$  would not be sufficient to explain the observed effective moments.<sup>39</sup> The observation of a full moment in the paramagnetic regime is somewhat surprising for a lower-valent, light actinide 5f ion, given the expected large crystal-field contribution to the term splittings relative to the spin–orbit interaction. Consistent with the form of the Curie–Weiss law expressed in eq 1, the negative Weiss temperatures are consistent with the antiferromagnetic interactions suggested by the cusps in the susceptibilities. The general magnitudes of the TIP contributions to the susceptibilities are also within the range expected for nonmetallic systems. The smaller value of the contribution measured for  $\text{Np}_3\text{S}_5$  compared to  $\text{Np}_3\text{Se}_5$  results in the offset of the two susceptibility curves (Figure 3). An understanding of the large difference in the  $\chi_0$  terms

determined for the two samples may lie in published resistivity measurements that show  $\text{Np}_3\text{S}_5$  to be a semiconductor whereas  $\text{Np}_3\text{Se}_5$  has an order of magnitude lower resistivity at 298 K and appears to be more semimetallic than semiconducting.<sup>18</sup> This suggests that the larger temperature-independent paramagnetic term for  $\text{Np}_3\text{Se}_5$  results from Pauli paramagnetism, which arises from a high density of states with a tendency for 5f band formation. Because the coordination environments for the two isostructural Np compounds are very similar, the difference in  $\chi_0$  is not the result of differences in crystal-field state energies. The larger (softer) selenide ion would be expected to have a larger overlap integral with the Np ions than would the sulfide ion. The implication of this result is the formation of enhanced Np–ligand bonding interactions in the selenide compound.

## Conclusions

The compounds  $\text{Np}_3\text{S}_5$  and  $\text{Np}_3\text{Se}_5$  are unique examples of mixed-valent binary neptunium chalcogenides containing both  $\text{Np}^{3+}$  and  $\text{Np}^{4+}$  cations. We have successfully prepared large single crystals of  $\text{Np}_3\text{S}_5$  and  $\text{Np}_3\text{Se}_5$  utilizing a CsCl flux. The structures of these isostructural compounds were redetermined by single-crystal X-ray diffraction methods. The results confirm those from earlier studies on powders but provide more accurate Np–S and Np–Se distances. Magnetic susceptibility measurements for  $\text{Np}_3\text{S}_5$  and  $\text{Np}_3\text{Se}_5$ , conducted on crushed single crystals, indicate that both compounds exhibit evidence for long-range antiferromagnetic orderings at low temperatures. Above the transition temperatures,  $\text{Np}_3\text{S}_5$  and  $\text{Np}_3\text{Se}_5$  behave as typical paramagnets. Their magnetic susceptibilities have been fit to a modified Curie–Weiss law with a larger temperature-independent paramagnetic contribution for the selenide over the sulfide. These results, which indicate that the Np–Se bonding interactions are stronger than are the Np–S interactions, are consistent with previous <sup>237</sup>Np Mössbauer studies and resistivity measurements on  $\text{Np}_3\text{S}_5$  and  $\text{Np}_3\text{Se}_5$ . Furthermore, the magnetic results for  $\text{Np}_3\text{S}_5$  and  $\text{Np}_3\text{Se}_5$  clarify their magnetic properties and provide some understanding of the interactions between magnetic cations in these compounds.

**Acknowledgment.** The research was supported at Northwestern University by the U.S. Department of Energy, Basic Energy Sciences, Chemical Sciences, Biosciences, and Geosciences Division and Division of Materials Sciences and Engineering Grant ER-15522 and at Argonne National Laboratory by the U.S. Department of Energy, OBES, Chemical Sciences and Engineering Division, under contract DEAC02-06CH11357.

**Supporting Information Available:** Crystallographic files in cif format for  $\text{Np}_3\text{S}_5$  and  $\text{Np}_3\text{Se}_5$ . This material is available free of charge via the Internet at <http://pubs.acs.org>.

(39) Staub, U.; Soderholm, L. In *Handbook on the Physics and Chemistry of Rare Earths*; Gschneidner, K. A., Jr., Eyring, LeR., Maple, M. B., Eds.; Elsevier: Amsterdam, 2000; Vol. 30, pp 491–545.